Pilot-scale production of peroxygenase from agrocybe aegerita

Tonin, Fabio; Tieves, Florian; Willot, Sébastien; Van Troost, Anouska; Van Oosten, Remco; Breestraat, Stefaan; Van Pelt, Sander; Alcalde, Miguel; Hollmann, Frank

DOI
10.1021/acs.oprd.1c00116

Publication date
2021

Document Version
Final published version

Published in
Organic Process Research and Development

Citation (APA)
Tonin, F., Tieves, F., Willot, S., Van Troost, A., Van Oosten, R., Breestraat, S., Van Pelt, S., Alcalde, M., & Hollmann, F. (2021). Pilot-scale production of peroxygenase from agrocybe aegerita. *Organic Process Research and Development*, *25*(6), 1414-1418. https://doi.org/10.1021/acs.oprd.1c00116

ORGANIC PROCESS RESEARCH & DEVELOPMENT
OPR&D

pubs.acs.org/OPRD

Article

Pilot-Scale Production of Peroxygenase from *Agrocybe aegerita*

Fabio Tonin,* Florian Tieves, Sébastien Willot, Anouska van Troost, Remco van Oosten, Stefaan Breestraat, Sander van Pelt, Miguel Alcalde, and Frank Hollmann*

Cite This: *Org. Process Res. Dev.* 2021, 25, 1414−1418

Read Online

ACCESS | Metrics & More | Article Recommendations | Supporting Information

ABSTRACT: The pilot-scale production of the peroxygenase from *Agrocybe aegerita* (r*Aae*UPO) is demonstrated. In a fed-batch fermentation of the recombinant *Pichia pastoris*, the enzyme was secreted into the culture medium to a final concentration of 0.29 g L^{-1} corresponding to 735 g of the peroxygenase in 2500 L of the fermentation broth after 6 days. Due to nonoptimized downstream processing, only 170 g of the enzyme has been isolated. The preparative usefulness of the so-obtained enzyme preparation has been demonstrated at a semipreparative scale (100 mL) as an example of the stereoselective hydroxylation of ethyl benzene. Using an adjusted H_2O_2 feed rate, linear product formation was observed for 7 days, producing more than 5 g L^{-1} (*R*)-1-phenyl ethanol. The biocatalyst performed more than 340.000 catalytic turnovers (942 g of the product per gram of r*Aae*UPO).

KEYWORDS: *biocatalysis, hydroxylation, peroxygenases, pilot-scale fermentation, specific oxyfunctionalization*

INTRODUCTION

Peroxygenases are receiving increased attention as selective oxyfunctionalization catalysts.[1] Compared to the well-known P450 monooxygenases, peroxygenases exhibit a significantly simpler molecular architecture and regeneration scheme. Both enzyme classes utilize an oxyferryl heme (compound I, Cpd I, Scheme 1c) as oxygenation species. Hence, in principle, all reactions that can be realized with P450 monooxygenases are also accessible through peroxygenases. P450 monooxygenases form Cpd I *via* reductive activation of molecular oxygen (Scheme 1a).[2] From a practical point of view, this mechanism brings about a range of challenges such as the orchestration of the complex electron transport chain and minimization of the undesired uncoupling reaction and the dependence on nicotinamide cofactors (together with appropriate regeneration systems).[3] Also, the poor solubility of molecular oxygen in aqueous reaction media poses a reaction engineering challenge.[4,5] In contrast, peroxygenases form Cpd I from hydrogen peroxide directly (Scheme 1b), thereby principally circumventing many issues occurring with P450 monooxygenases.

Scheme 1. Comparison of the Overall Reaction Schemes of P450 Monooxygenase- (a) and Peroxygenase-Catalyzed Oxyfunctionalization Reactions (b); (c) Structure of the Oxygen-Transferring Heme Species (Compound I, Cpd I)

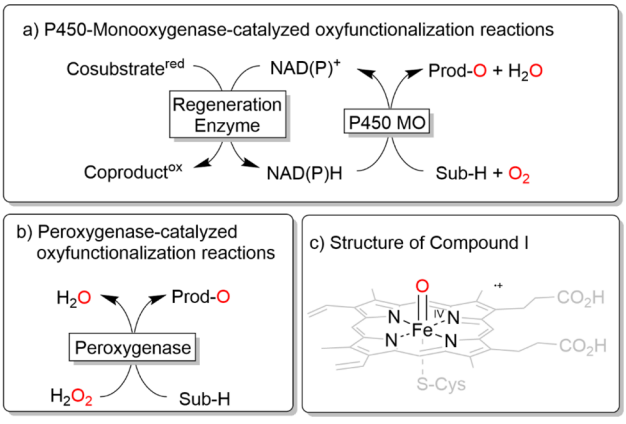

As a consequence of the simpler reaction mechanism, peroxygenases appear to be promising alternatives to the established P450 monooxygenases.

Nevertheless, a range of challenges still need to be addressed en route to peroxygenases becoming truly practical catalysts for selective oxyfunctionalization chemistry. First, the number of peroxygenase variants with tailored selectivity for a broader range of starting materials must be increased. Second, the H_2O_2-dependence of peroxygenases also bears the challenge of irreversible oxidative inactivation of the biocatalyst. Finally, concepts for the large-scale application are so far poorly developed.

The first issue currently can be addressed by enlarging the portfolio of peroxygenases by new examples from natural and manmade diversity.[6−16] The stability issue can also be considered to be principally solved as a broad range of *in situ* H_2O_2 generation systems are now available to provide the peroxygenase catalysts with the appropriate amounts of H_2O_2 to maximize their catalytic activity while minimizing the undesired oxidative inactivation.[17]

In the current contribution, we aimed at demonstrating the scalability of peroxygenase fermentation at a pilot scale. For

Received: April 2, 2021
Published: June 9, 2021

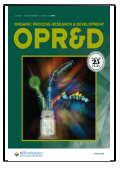

Scheme 2. Process Scheme of the Pilot-Scale Production of r*Aae*UPO Reported in This Contribution

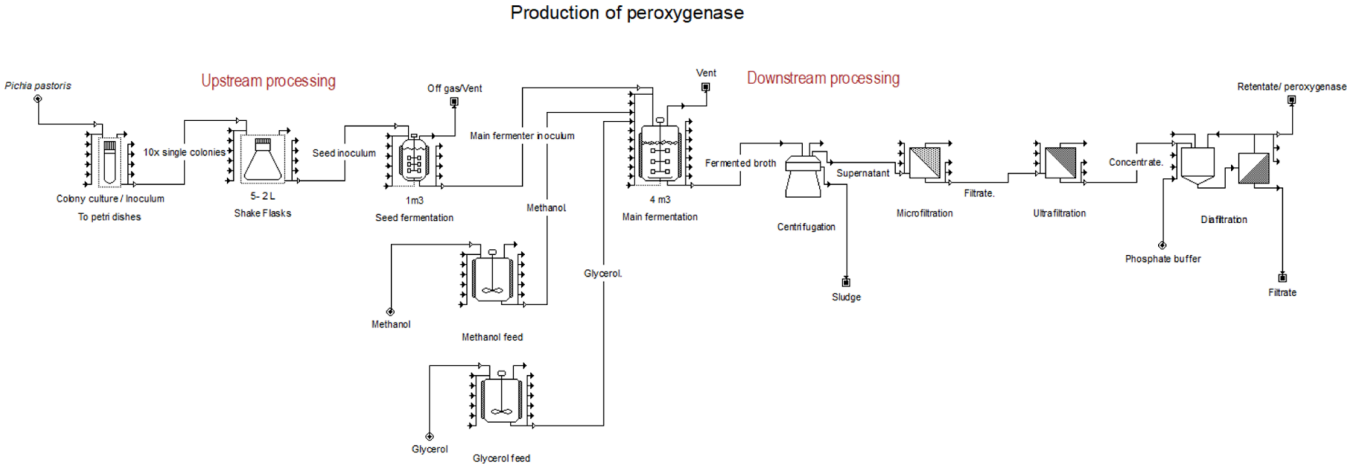

this, we chose the evolved, recombinant peroxygenase from *Agrocybe aegerita* (r*Aae*UPO),[7,12,18] which so far has been produced at fermentation scales of up to 10 L.[19]

RESULTS

To initiate the pilot-scale fermentation, several preculture fermentations were performed, also known as seed train, in order to attain a suitable inoculation culture (Scheme 2).

In brief, recombinant *Pichia pastoris* (X-33) expressing r*Aae*UPO was grown on YPD-agar (containing 100 μg × mL^{-1} Zeocin).[20] After 2 days incubation at 30 °C, 10 individual colonies were used to inoculate five 500 mL scale precultures (BMGY medium).[21] Overnight incubation in a rotary shaker (140 rpm, 30 °C) resulted in precultures having reached the stationary phase with an optical density (OD_{600}) of approx. 10. The combined precultures were used to inoculate the seed culture fermentation (250 L BMGY medium), which was incubated for 24 h (30 °C, 200 rpm, aeration at 0.5 vvm), reaching a cell density (OD_{600}) of 16 (Supporting Information Sections 1.1 and 1.2).

The main fermentation (Supporting Information Section 1.3) was performed using a 4 m^3 fermenter filled with 1500 L of BMGY medium supplemented with *Pichia* trace metal solution (12 g L^{-1} PTM1 trace solution) adjusted to pH 5 with NH_4OH solution (28%) and containing 4% (v/v) glycerol. This medium was inoculated with a 75 kg fraction of the seed fermentation broth (attaining an initial OD_{600} of approx. 1). After the initial glycerol had been consumed (after approx. 18 h), additional glycerol feed (20 L h^{-1} of a 545 g L^{-1} stock) was initiated and the biomass concentration further increased from OD_{600} 52 to 190. Afterward, the glycerol feed was stopped and r*Aae*UPO expression was induced by starting methanol feeding (starting with a bolus of 9 kg MeOH) at a rate of 4.5 kg_{MeOH} h^{-1} (approx. 5.7 L h^{-1}, Figure S7). At this stage, the fermenter temperature was lowered to 25 °C. It is important to mention here that the oxygen saturation of the fermentation broth was maintained around 20% by adjusting the stirring speed or (if necessary) the aeration flow (Figure S4). The production of r*Aae*UPO was monitored by sampling the culture broth and quantifying the enzyme activity in the ABTS assay (Figure 1). In the first 48 h after initiation of the induction, the r*Aae*UPO activity increased relatively slowly but sped-up during the next 48 h (after the accumulation of biomass had ceased), reaching a saturation level of approx. 300 U_{ABTS} mL^{-1}.

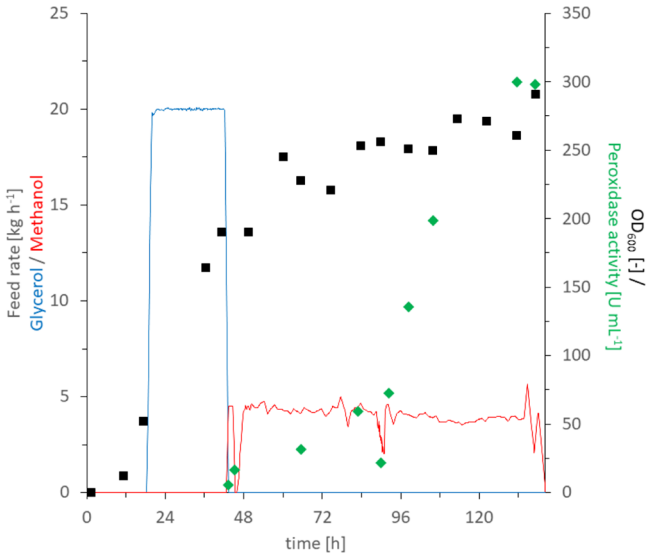

Figure 1. Time profile of the main fermentation. Black squares: biomass as determined *via* the optical density at 600 nm, green diamonds: r*Aae*UPO$_{ABTS}$ activity determined *via* the ABTS assay, blue line: smoothed glycerol feeding profile, red line: smoothed MeOH feeding profile.

After the r*Aae*UPO accumulation had ceased (at 298 U_{ABTS} mL^{-1} corresponding to 738 M U_{ABTS} or 735 g of r*Aae*UPO), the fermentation broth was cooled down to 10 °C. At this point, the fermentation broth (2484 kg) contained approx. 33% (v/v) of biomass. Therefore, the broth was diluted with 3000 L of water and centrifuged, obtaining 3642 L of the supernatant (still containing 0.38% (w/v) biomass) with a r*Aae*UPO content of 337 g (45.9% yield). The residual 1841 L (still containing approx. 60% v/v of the supernatant) for technical reasons had to be discarded (*vide infra*).

To remove the residual biomass in the supernatant, it was submitted to a microfiltration step (K700 disc filter with an average pore size of 6−15 μm). During this step, approx. 13% of the biocatalyst was lost, adding up to an overall yield of 40% (294 g r*Aae*UPO). Finally, the enzyme solution was further concentrated *via* ultrafiltration (30 kDa GE Healthcare UFP-30-E-85 membrane) and rebuffered to 0.2 mM KPi buffer pH 7 in a diafiltration step.

https://doi.org/10.1021/acs.oprd.1c00116
Org. Process Res. Dev. 2021, 25, 1414−1418

Overall, 76.3 L of a concentrated r*Aae*UPO solution was obtained with an r*Aae*UPO concentration (as determined *via* the CO-differential spectra) of 43 μM. The solution was shock-frozen by adding it dropwise into liquid nitrogen and stored at −20 °C until further use. The overall enzyme yield (170 g) was 23%. The enzyme preparation contained approx. 2.5 gL^{-1} of r*Aae*UPO, corresponding to more than 85% of the overall protein content (Supporting Information Section 2). Table 1 summarizes the key parameters of the downstream processing (DSP) steps and illustrates the enzyme losses in the individual processing steps.

Table 1. Summary of the DSP Steps

	volume [L]	m(r*Aae*UPO) [g]	$yield_{step}$ [%]	$yield_{total}$ [%]
end of the fermentation	2484	735	100.0	100.0
cool-down and dilution	5484	735	100.0	100.0
centrifugation (supernatant)	3642	337	45.9	45.9
microfiltration	3642	294	87.2	40.0
concentration and diafiltration	76.3	170	57.8	23.1

To test the catalytic performance of the r*Aae*UPO obtained from the pilot-scale fermentation, we used it for the hydroxylation of ethyl benzene to (*R*)-1-phenyl ethanol at a semipreparative scale (100 mL). For this, we used a two-liquid-phase-system approach (2LPS) with an aqueous, r*Aae*UPO-containing, reaction phase and ethyl benzene as the organic phase serving as the substrate reservoir and product sink (Scheme 3). For reasons of simplicity, H_2O_2 as an oxidant was fed to the emulsion externally.

Scheme 3. r*Aae*UPO-Catalyzed Stereoselective Hydroxylation of Ethyl Benzene to (*R*)-1-Phenyl Ethanol Using a 2LPS Approach

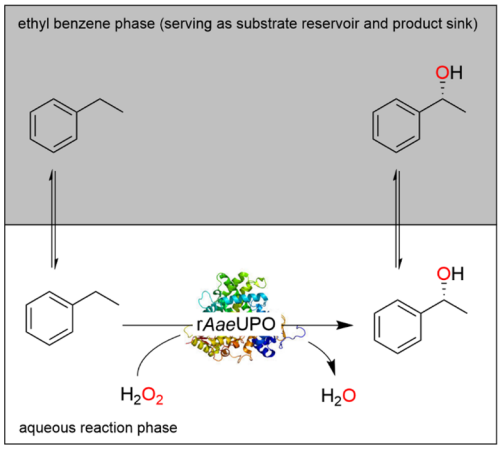

In this experiment, the r*Aae*UPO concentration in the aqueous reaction phase was 0.5 μM and a H_2O_2 dosing rate of 49 mmol h^{-1} was applied (0.6 mL of an 82 mM stock solution). The H_2O_2 dose rate was chosen conservatively to minimize the undesired oxidative degradation of r*Aae*UPO.[17] As shown in Figure 2, this approach enabled the stable accumulation of the desired product (*R*)-1-phenyl ethanol over at least 7 days, resulting in a final product concentration of 120 mM (14.4 g L^{-1}) of the desired product in the organic layer. Within the aqueous layer, (*R*)-1-phenyl ethanol accumulated

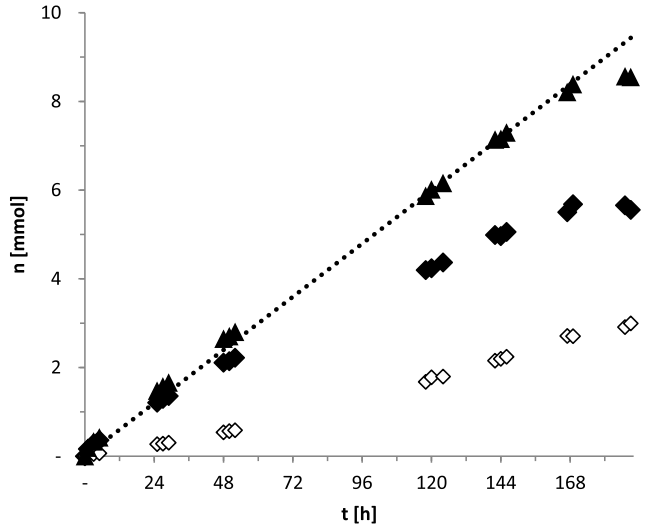

Figure 2. Time course of the semipreparative-scale hydroxylation of ethyl benzene to (*R*)-1-phenyl ethanol. Reaction conditions: the initial reaction mixture consisted of 50 mL of ethyl benzene and 50 mL of phosphate buffer (100 mM, pH 7) containing 500 nM biocatalyst. The reaction was thermostatted at 25 °C and stirred continuously at 150 rpm. H_2O_2 added continuously at a rate of 49 mmol h^{-1} was applied (0.6 mL of a 82 mM stock solution), triangles: total product formed (sum of product amounts in the aqueous and organic layer), filled diamonds: (*R*)-1-phenyl ethanol found in the organic layer, open diamonds: (*R*)-1-phenyl ethanol found in the aqueous layer, dotted line: amount of H_2O_2 added to the reactor over time.

to approximately 20 mM (saturation concentration in aqueous media) within 7 days. Please note that throughout the experiment, the volume of the aqueous layer increased to approx. 150 mL, thereby explaining the apparent discrepancy between the 6 times higher concentration in the organic layer and only roughly twofold higher absolute amount. It is worth mentioning that from approx. 48 h onward, traces of acetophenone (stemming from the r*Aae*UPO-catalyzed oxidation of (*R*)-1-phenyl ethanol) were also found in the organic phase.

Throughout the experiment, aqueous-layer samples were qualitatively analyzed for H_2O_2, showing no detectable H_2O_2 until 167 h. This corresponds well to the total amount of the product formed and the amount of H_2O_2 added to the reactor. Hence, we conclude that H_2O_2 was the overall rate-limiting component in the reaction setup. After 167 h, a gradual increase of H_2O_2 was observed, together with the ceasing product accumulation, which we attribute to the final inactivation of the biocatalyst.

In total, 8.5 mmol of (*R*)-1-phenyl ethanol (1.04 g) was formed using 1.1 mg of r*Aae*UPO. This corresponds to a product-to-catalyst ratio of 942 $g_{Product} \times g_{rAaeUPO}^{-1}$ or a turnover number of 340.000 for the biocatalyst. The volumetric productivity of the system was 60 $mg_{Product}\ L^{-1} \times h^{-1}$, corresponding to an average turnover frequency of the biocatalyst of 0.56 s^{-1} over 168 h.

DISCUSSION

In the main fermentation, approx. 735 g of r*Aae*UPO has been produced in 2480 L of fermentation broth. It is interesting to note that r*Aae*UPO accumulation only started approx. 48 h after the start of the methanol induction phase and coincided

https://doi.org/10.1021/acs.oprd.1c00116
Org. Process Res. Dev. 2021, 25, 1414−1418

with the end of biomass accumulation. At present, we lack a plausible explanation for this comparably long lag time between initiation of the methanol induction and r*Aae*UPO expression, which has also been observed in previous studies on 10 L.[18]

The final r*Aae*UPO titer of 0.29 $g_{rAaeUPO}\ L_{fermentation\ broth}^{-1}$ corresponds well to the r*Aae*UPO expression levels (217 mg L^{-1}) reported previously for this expression system at the 10 L scale.[18] Possibly, improved expression systems will enable higher peroxygenase expression levels.

Out of the overall 735 g of r*Aae*UPO produced, only 170 g of the enzyme has actually been recovered. The major bottleneck in the downstream procedure was the first centrifugation step: using the semicontinuous centrifuge resulted in a low recovery of the supernatant (~50%) containing the r*Aae*UPO. This was due to the inability of the centrifuge to separate the high-solid-loaded broth obtained at the end of the fermentation. The single pass yield could be improved to ~70% by using a nozzle-mode continuous centrifuge. Resuspension of the sludge and a second pass could increase the yield to ~95%. However, higher dilution of the enzyme titer and longer processing times would be expected.

Notably, the inefficient centrifugation step caused several problems in the subsequent micro- and ultrafiltration steps, causing the clogging of the filters that had to be washed several times during these processes. A tangential-flow microfiltration should be used to remove the leftover organisms from the obtained supernatant from the centrifugation step (also known as the polishing step). By using this technology, the yield of this step can be increased to ~95% but again leading to longer processing times. The freeze-drying of the supernatant could represent an alternative solution, leading to the procurement of the lyophilized enzyme (as powder) that can be easily stored and transported.

In conclusion, we are confident that higher recovery yield (80−90%) can be achieved by tailoring an optimized DSP process. However, the effect of longer processing times and the implementation of additional steps should be taken into consideration while evaluating the production cost of r*Aae*UPO.

The biotransformation results underline the preparative potential of peroxygenases. To the best of our knowledge, the turnover numbers achieved here range among the highest reported so far for an enzymatic oxyfunctionalization catalyst and point toward economically feasible application.[22] Compared to similar, P450—monooxygenase-catalyzed reactions, further advantages are the much simpler reaction setups avoiding nicotinamide cofactors and corresponding regeneration systems, as well as stoichiometric amounts of gluconate byproducts.[23,24]

The volumetric productivity of the biotransformation shown here was admittedly rather low. This was due to the rather low H_2O_2 feeding rate, which was chosen to maximize the robustness of the biocatalyst. More courageous feeding strategies may result in higher, industrially more interesting space time yields. Another issue of the external H_2O_2 addition strategy, however, also lies with the significant dilution of the reaction mixture (increasing from initially 100 mL to approx. 200 mL after 7 days). Further developments therefore will focus on the application of *in situ* H_2O_2 generation from O_2 using simple reductants such as formate[25−27] or methanol.[28−30]

Overall, in this contribution, we have demonstrated that peroxygenases can be produced at least at the pilot scale, yielding practical amounts of these promising catalysts for organic oxyfunctionalization chemistry.

■ ASSOCIATED CONTENT

Supporting Information

The Supporting Information is available free of charge at https://pubs.acs.org/doi/10.1021/acs.oprd.1c00116.

Detailed descriptions of the fermentation procedures, the enzymatic hydroxylation reaction, and further analytical data (PDF)

■ AUTHOR INFORMATION

Corresponding Authors

Fabio Tonin − *Department of Biotechnology, Delft University of Technology, 2629HZ Delft, The Netherlands;* orcid.org/0000-0002-5358-5271; Email: f.tonin@tudelft.nl

Frank Hollmann − *Department of Biotechnology, Delft University of Technology, 2629HZ Delft, The Netherlands;* orcid.org/0000-0003-4821-756X; Email: f.hollmann@tudelft.nl

Authors

Florian Tieves − *Department of Biotechnology, Delft University of Technology, 2629HZ Delft, The Netherlands;* orcid.org/0000-0002-6821-4190

Sébastien Willot − *Department of Biotechnology, Delft University of Technology, 2629HZ Delft, The Netherlands;* orcid.org/0000-0001-8086-0876

Anouska van Troost − *Department of Biotechnology, Delft University of Technology, 2629HZ Delft, The Netherlands;* orcid.org/0000-0002-2358-4016

Remco van Oosten − *Department of Biotechnology, Delft University of Technology, 2629HZ Delft, The Netherlands;* orcid.org/0000-0002-3850-6125

Stefaan Breestraat − *Bioprocess Pilot Facility B.V., 2613 AX Delft, The Netherlands;* orcid.org/0000-0002-9013-7566

Sander van Pelt − *Bioprocess Pilot Facility B.V., 2613 AX Delft, The Netherlands;* orcid.org/0000-0003-3311-3848

Miguel Alcalde − *Department of Biocatalysis, Institute of Catalysis, 28049 Madrid, Spain;* orcid.org/0000-0001-6780-7616

Complete contact information is available at: https://pubs.acs.org/10.1021/acs.oprd.1c00116

Author Contributions

The manuscript was written through contributions of all authors. All authors have given approval to the final version of the manuscript.

Funding

Funding by the European Research Commission (ERC consolidator grant no. 648026) is gratefully acknowledged.

Notes

The authors declare no competing financial interest.

■ REFERENCES

(1) Hobisch, M.; Holtmann, D.; de Santos, P. G.; Alcalde, M.; Hollmann, F.; Kara, S. Recent developments in the use of peroxygenases − Exploring their high potential in selective oxy-

functionalisations. *Biotechnol. Adv.* **2020**, DOI: 10.1016/j.biotechadv.2020.107615.
(2) Urlacher, V. B.; Girhard, M. Cytochrome P450 monooxygenases: an update on perspectives for synthetic application. *Trends Biotechnol.* **2012**, *30*, 26−36.
(3) Holtmann, D.; Hollmann, F. The Oxygen Dilemma: A Severe Challenge for the Application of Monooxygenases? *ChemBioChem* **2016**, *17*, 1391−1398.
(4) Dias Gomes, M.; Bommarius, B. R.; Anderson, S. R.; Feske, B. D.; Woodley, J. M.; Bommarius, A. S. Bubble Column Enables Higher Reaction Rate for Deracemization of (R,S)-1-Phenylethanol with Coupled Alcohol Dehydrogenase/NADH Oxidase System. *Adv. Synth. Catal.* **2019**, *361*, 2574−2581.
(5) Lundemo, M. T.; Woodley, J. M. Guidelines for development and implementation of biocatalytic P450 processes. *Appl. Microbiol. Biotechnol.* **2015**, *99*, 2465−2483.
(6) Martínez, A. T.; Ruiz-Dueñas, F. J.; Gutiérrez, A.; del Río, J. C.; Alcalde, M.; Liers, C.; Ullrich, R.; Hofrichter, M.; Scheibner, K.; Kalum, L.; Vind, J.; Lund, H. Search, engineering, and applications of new oxidative biocatalysts. *Biofuels, Bioprod. Biorefin.* **2014**, *8*, 819−835.
(7) Molina-Espeja, P.; Garcia-Ruiz, E.; Gonzalez-Perez, D.; Ullrich, R.; Hofrichter, M.; Alcalde, M. Directed Evolution of Unspecific Peroxygenase from Agrocybe aegerita. *Appl. Environ. Microbiol.* **2014**, *80*, 3496−3507.
(8) Molina-Espeja, P.; Cañellas, M.; Plou, F. J.; Hofrichter, M.; Lucas, F.; Guallar, V.; Alcalde, M. Synthesis of 1-Naphthol by a Natural Peroxygenase Engineered by Directed Evolution. *ChemBioChem* **2016**, *17*, 341−349.
(9) Molina-Espeja, P.; de Santos, P. G.; Alcalde, M. In *Directed Enzyme Evolution: Advances and Applications*; Alcalde, M., Ed.; Springer International Publishing: Cham, 2017, pp 127−143.
(10) Gomez de Santos, P.; Cervantes, F. V.; Tieves, F.; Plou, F. J.; Hollmann, F.; Alcalde, M. Benchmarking of laboratory evolved unspecific peroxygenases for the synthesis of human drug metabolites. *Tetrahedron* **2019**, *75*, 1827−1831.
(11) Gomez de Santos, P.; Lazaro, S.; Viña-Gonzalez, J.; Hoang, M. D.; Sánchez-Moreno, I.; Glieder, A.; Hollmann, F.; Alcalde, M. Evolved Peroxygenase−Aryl Alcohol Oxidase Fusions for Self-Sufficient Oxyfunctionalization Reactions. *ACS Catal.* **2020**, *10*, 13524−13534.
(12) Ullrich, R.; Nüske, J.; Scheibner, K.; Spantzel, J.; Hofrichter, M. Novel haloperoxidase from the agaric basidiomycete Agrocybe aegerita oxidizes aryl alcohols and aldehydes. *Appl. Environ. Microbiol.* **2004**, *70*, 4575−4581.
(13) Ullrich, R.; Liers, C.; Schimpke, S.; Hofrichter, M. Purification of homogeneous forms of fungal peroxygenase. *Biotechnol. J.* **2009**, *4*, 1619−1626.
(14) Hofrichter, M.; Ullrich, R.; Pecyna, M. J.; Liers, C.; Lundell, T. New and classic families of secreted fungal heme peroxidases. *Appl. Microbiol. Biotechnol.* **2010**, *87*, 871−897.
(15) Kellner, H.; Luis, P.; Pecyna, M. J.; Barbi, F.; Kapturska, D.; Krüger, D.; Zak, D. R.; Marmeisse, R.; Vandenbol, M.; Hofrichter, M. Widespread Occurrence of Expressed Fungal Secretory Peroxidases in Forest Soils. *PLoS One* **2014**, *9*, No. e95557.
(16) Babot, E. D.; del Río, J. C.; Cañellas, M.; Sancho, F.; Lucas, F.; Guallar, V.; Kalum, L.; Lund, H.; Gröbe, G.; Scheibner, K.; Ullrich, R.; Hofrichter, M.; Martínez, A. T.; Gutiérrez, A. Steroid Hydroxylation by Basidiomycete Peroxygenases: a Combined Experimental and Computational Study. *Appl. Environ. Microbiol.* **2015**, *81*, 4130−4142.
(17) Burek, B. O.; Bormann, S.; Hollmann, F.; Bloh, J. Z.; Holtmann, D. Hydrogen peroxide driven biocatalysis. *Green Chem.* **2019**, *21*, 3232−3249.
(18) Molina-Espeja, P.; Ma, S.; Mate, D. M.; Ludwig, R.; Alcalde, M. Tandem-yeast expression system for engineering and producing unspecific peroxygenase. *Enzyme Microb. Technol.* **2015**, *73*−*74*, 29−33.
(19) Tieves, F.; Tonin, F.; Fernández-Fueyo, E.; Robbins, J. M.; Bommarius, B.; Bommarius, A. S.; Alcalde, M.; Hollmann, F. Energising the E-factor: The E^+-factor. *Tetrahedron* **2019**, *75*, 1311−1314.
(20) Sherman, F. *Methods in Enzymology*; Guthrie, C., Fink, G. R., Eds.; Academic Press, 2002; Vol. *350*, pp 3−41.
(21) Basanta, A.; Gómez-Sala, B.; Sánchez, J.; Diep, D. B.; Herranz, C.; Hernández, P. E.; Cintas, L. M. Use of the Yeast Pichia pastoris as an Expression Host for Secretion of Enterocin L50, a Leaderless Two-Peptide (L50A and L50B) Bacteriocin from Enterococcus faecium L50. *Appl. Environ. Microbiol.* **2010**, *76*, 3314−3324.
(22) Tufvesson, P.; Lima-Ramos, J.; Nordblad, M.; Woodley, J. M. Guidelines and cost analysis for catalyst production in biocatalytic processes. *Org. Process Res. Dev.* **2010**, *15*, 266−274.
(23) Kaluzna, I.; Schmitges, T.; Straatman, H.; van Tegelen, D.; Müller, M.; Schürmann, M.; Mink, D. Enabling Selective and Sustainable P450 Oxygenation Technology. Production of 4-Hydroxy-alpha-isophorone on Kilogram Scale. *Org. Process Res. Dev.* **2016**, *20*, 814−819.
(24) Neufeld, K.; Marienhagen, J.; Schwaneberg, U.; Pietruszka, J. Benzylic hydroxylation of aromatic compounds by P450 BM3. *Green Chem.* **2013**, *15*, 2408−2421.
(25) van Schie, M. M. C. H.; Zhang, W.; Tieves, F.; Choi, D. S.; Park, C. B.; Burek, B. O.; Bloh, J. Z.; Arends, I. W. C. E.; Paul, C. E.; Alcalde, M.; Hollmann, F. Cascading g-C3N4 and Peroxygenases for Selective Oxyfunctionalization Reactions. *ACS Catal.* **2019**, *9*, 7409−7417.
(26) Tieves, F.; Willot, S. J. P.; van Schie, M. M. C. H.; Rauch, M. C. R.; Younes, S. H. H.; Zhang, W.; Dong, J.; Gomez de Santos, P.; Robbins, J. M.; Bommarius, B.; Alcalde, M.; Bommarius, A. S.; Hollmann, F. Formate oxidase (FOx) from Aspergillus oryzae: one catalyst to promote H_2O_2-dependent biocatalytic oxidation reactions. *Angew. Chem., Int. Ed.* **2019**, *58*, 7873−7877.
(27) Pesic, M.; Willot Sébastien, J.-P.; Fernández-Fueyo, E.; Tieves, F.; Alcalde, M.; Hollmann, F. Multienzymatic in situ hydrogen peroxide generation cascade for peroxygenase-catalysed oxyfunctionalisation reactions. *Z. Naturforsch., C: J. Biosci.* **2019**, *74*, 101.
(28) Yuan, B.; Mahor, D.; Fei, Q.; Wever, R.; Alcalde, M.; Zhang, W.; Hollmann, F. Water-Soluble Anthraquinone Photocatalysts Enable Methanol-Driven Enzymatic Halogenation and Hydroxylation Reactions. *ACS Catal.* **2020**, *10*, 8277−8284.
(29) Willot, S. J. P.; Hoang, M. D.; Paul, C. E.; Alcalde, M.; Arends, I. W. C. E.; Bommarius, A. S.; Bommarius, B.; Hollmann, F. FOx News Towards Methanol-driven Biocatalytic Oxyfunctionalisation Reactions. *ChemCatChem* **2020**, *12*, 2713−2716.
(30) Zhang, W.; Burek, B. O.; Fernández-Fueyo, E.; Alcalde, M.; Bloh, J. Z.; Hollmann, F. Selective activation of C-H bonds by cascading photochemistry with biocatalysis. *Angew. Chem.* **2017**, *56*, 15451−15455.

https://doi.org/10.1021/acs.oprd.1c00116
Org. Process Res. Dev. 2021, 25, 1414−1418